processes

MDPI

Article

Study on Adsorption and Photocatalytic Properties of Zinc Ferrite

Jinlin Yang [1], Xingnan Huo [1], Zongyu Li [1], Hengjun Li [2], Teng Wang [1] and Shaojian Ma [1,*]

[1] State Key Laboratory of Featured Metal Materials and Life-Cycle Safety for Composite Structures, MOE Key Laboratory of New Processing Technology for Nonferrous Metals, Guangxi Higher School Key Laboratory of Minerals Engineering and Materials, College of Resources, Environment and Materials, Guangxi University, Nanning 530004, China
[2] College of Chemistry and Chemical Engineering, Guangxi University, Nanning 530004, China
* Correspondence: 1615391004@alu.gxu.edu.cn; Tel.: +86-131-5266-0958

Abstract: In this study, methyl orange, methylene blue, and amido black 10B were removed as target dyes using purified, synthetic, and purchased zinc ferrite as adsorbents and photocatalysts. The highest removal rates of amido black 10B by these adsorbents ranged from 81.62% to 88.33%. The removal rate of methyl orange was approximately 1%, and the removal rate of methylene blue was approximately 2%. Hence, an investigation was conducted to elucidate the factors that influence the removal efficacy of purified zinc ferrite on amido black 10B. Titanium dioxide prepared at different calcination temperatures was unsuccessful in removing amido black 10B, but the physical mixing of titanium dioxide prepared at suitable calcination temperatures with purified zinc ferrite had a positive effect on amido black 10B removal. Since zinc ferrite could not be used as an adsorbent to remove methyl orange and methylene blue, the photocatalytic degradation properties of zinc ferrite and its influencing factors were studied. The optimal conditions for the photocatalytic degradation of methylene blue and methyl orange by zinc ferrite are as follows: a zinc ferrite catalyst dosage of 0.15 g, an initial solution concentration of 20 mg/L, and a pH of 6.0. The dosage of the zinc ferrite/titanium dioxide composite catalyst is 0.15 g, the initial solution concentration is 20 mg/L, and the pH is 6.5.

Keywords: zinc ferrite; adsorption; photocatalysis; amido black 10B; methyl orange; methylene blue

Citation: Yang, J.; Huo, X.; Li, Z.; Li, H.; Wang, T.; Ma, S. Study on Adsorption and Photocatalytic Properties of Zinc Ferrite. *Processes* **2023**, *11*, 1607. https://doi.org/10.3390/pr11061607

Academic Editors: María José Martín de Vidales, Alessandro Navarra, Norman Toro, Roberto Parra and Henrik Saxen

Received: 19 April 2023
Revised: 21 May 2023
Accepted: 23 May 2023
Published: 24 May 2023

1. Introduction

Dye wastewater is wastewater discharged during the production of dyes and pigments obtained from benzene, toluene, and naphthalene as raw materials through nitrification and iodization to produce intermediates, which undergo diazotization, coupling, and vulcanization reactions. Dye wastewater is characterized by a large water volume, high concentration, complex components, deep chrominance, high organic pollutant content, large water quality variations, high biological toxicity, and biodegradation difficulties. Thus, it is classified as an organic wastewater that is difficult to treat. Dyes possess strong photolysis and oxidation resistances and contain various organic compounds with biological toxicity or "three cause" (carcinogenic, teratogenic, and mutagenic) properties [1]. Therefore, without any purification treatment, they would cause serious environmental problems and even threaten human life, health, and safety. Therefore, efficient dye wastewater treatment is crucial. Dispersing dyes include azo and non-azo dyes, among which 75% are azo dyes [2]. Many types of dispersing dyes are known, with methyl orange, methylene blue, and amido black 10B being representative examples. To date, various dye wastewater treatment methods have been developed. Dye wastewater treatment methods are mainly divided into three types: physical, chemical, and biological methods; combinations of the three types of treatment methods are also used. Physical methods mainly include adsorption, ion exchange, and membrane filtration [3,4]. Chemical methods mainly include chemical oxidation, advanced oxidation technology, the Fenton reagent method,

and photocatalytic oxidation [5–8]. Biological methods mainly include anaerobic microbial and aerobic biological methods and anaerobic–aerobic biological combinations [9–11]. In short, adsorption consists of the use of an adsorbent with a large specific surface area, a pore-rich structure, and polar groups; the target pollutant molecules become attached to the adsorbent and are thus removed to effectively degrade pollutants. Photocatalysis technology is a green treatment method that uses the photochemical reaction between a catalyst and various organic materials on its surface under light irradiation. In the process, organic pollutants are decomposed into small inorganic molecules, such as CO_2, H_2O, HX, and minerals, through oxidation–reduction reactions. Zinc ferrite is also known as spinel ferrite. Spinel ferrites can be divided into positive spinel, inverse spinel, and mixed spinel according to differences in the positions of cations in the crystal structure. Normally, zinc ferrite is in the form of orthospinel ferrite. Zinc ferrite has excellent properties and wide applications. Zinc ferrite has good soft magnetic properties, wave absorption, high-temperature resistance, corrosion resistance, non-toxic characteristics, catalytic performance, and photoelectric conversion performance [12–15]. Additionally, titanium dioxide is also a semiconductor, with stable chemical properties, strong photostability, and high oxidation efficiency; importantly, it is also non-toxic and environmentally friendly. Thus, zinc ferrite can be used as a photocatalyst and adsorbent, and titanium dioxide can be used as a photocatalyst to degrade organic matter through photocatalysis. For example, Cai et al. [16] synthesized a visible-light-responsive photocatalyst through the reduction–oxidation method. The decolorization rate of Orange II in the visible/$ZnFe_2O_4$/H_2O_2 system was high, which indicated that $ZnFe_2O_4$ had high photocatalytic activity for Orange II degradation in visible light. Savunthari et al. [17] reported that doped and co-doped zinc ferrite magnetic nanoparticles were successfully synthesized through the solution combustion technique. It was found that co-doped zinc ferrite ($Zn_{0.50}Cu_{0.50}Fe_{1.90}Bi_{0.10}O_4$ and $Zn_{0.50}Cu_{0.50}Fe_{1.95}Ce_{0.05}O_4$) nanoparticles exhibited a higher bisphenol A removal efficiency than the doped and un-doped zinc ferrite nanoparticles. Li et al. [18] successfully synthesized a visible-light-driven Ag/AgBr/$ZnFe_2O_4$ photocatalyst via a deposition–precipitation and photoreduction method. The prepared Ag/AgBr/$ZnFe_2O_4$ nanocomposites exhibited high photocatalytic activities for the degradation of gaseous toluene and MO. The Ag/AgBr/$ZnFe_2O_4$ nanocomposite was stable and could be effectively recovered easily in solution with a magnet. As can be seen from the above, relevant studies mainly focus on zinc ferrite as a photocatalyst for dye degradation, while the use of zinc ferrite as an adsorbent for dye removal is relatively rare. At the same time, these studies are based on synthetic zinc ferrite, and the properties of purified zinc ferrite in adsorption or photocatalytic dyes are rarely reported. In this study, methylene blue (Hln), methyl orange (MB), and amido black 10B (AB 10B) dispersing dyes were selected as the target removal materials. Based on the research on the properties and differences between different types of zinc ferrite, such as purified, synthetic, and purchased zinc ferrite, and physical mixtures or complexes with titanium dioxide, the target dyes were treated through adsorption and photocatalysis to study their adsorption and photocatalytic properties. The effects of the initial concentrations of target dyes, the initial pH value, adsorbent particle size, and other factors on the removal performance of zinc ferrite were explored. In addition, the effects of the dye type, zinc ferrite type, initial concentration of the solution, and other factors on photocatalytic degradation were explored. This study paves the way for developing a new process for the production of zinc ferrite with industrial application value and for the efficient treatment of dye wastewater.

2. Materials and Methods

2.1. Preparation of Zinc Ferrite, Titanium Dioxide, and Their Composites

Zinc ferrite was obtained from zinc calcine and sulfuric acid. Zinc ferrite was synthesized with ferric nitrate nonahydrate, zinc nitrate hexahydrate, and sodium hydroxide as the raw materials. Titanium dioxide was synthesized using titanium oxide sulfate and ammonia water. Finally, composites of purified zinc ferrite and titanium dioxide were

prepared from purified zinc ferrite, titanium oxide sulfate, and ammonia water [19]. The test samples described above are listed in Table 1.

Table 1. Preparation of experimental samples and their numbers.

Main Material	Roasting Temperature/°C	Product	Product Number
Zinc calcine + H_2SO_4	/	$ZnFe_2O_4$ + $PbSO_4$	PZ
Fe $(NO_3)_3 \cdot 9H_2O$ + Zn $(NO_3)_2 \cdot 6H_2O$	400	$ZnFe_2O_4$	SZ400
Fe $(NO_3)_3 \cdot 9H_2O$ + Zn $(NO_3)_2 \cdot 6H_2O$	500	$ZnFe_2O_4$	SZ500
Fe $(NO_3)_3 \cdot 9H_2O$ + Zn $(NO_3)_2 \cdot 6H_2O$	600	$ZnFe_2O_4$	SZ600
Fe $(NO_3)_3 \cdot 9H_2O$ + Zn $(NO_3)_2 \cdot 6H_2O$	700	$ZnFe_2O_4$	SZ700
$TiOSO_4$ + $NH_3 \cdot H_2O$	300	TiO_2	T300
$TiOSO_4$ + $NH_3 \cdot H_2O$	400	TiO_2	T400
$TiOSO_4$ + $NH_3 \cdot H_2O$	500	TiO_2	T500
$TiOSO_4$ + $NH_3 \cdot H_2O$	600	TiO_2	T600
$TiOSO_4$ + $NH_3 \cdot H_2O$	700	TiO_2	T700
$TiOSO_4$ + $NH_3 \cdot H_2O$ + 5%PZ	400	$ZnFe_2O_4/TiO_2$	T400/PZ (5%)
$TiOSO_4$ + $NH_3 \cdot H_2O$ + 5%PZ	500	$ZnFe_2O_4/TiO_2$	T500/PZ (5%)
$TiOSO_4$ + $NH_3 \cdot H_2O$ + 10%PZ	500	$ZnFe_2O_4/TiO_2$	T500/PZ (10%)
$ZnFe_2O_4$	/	$ZnFe_2O_4$	BZ

2.2. Adsorption Experiments

The UV–visible absorption spectra of 20 mg/L solutions of methyl orange, methylene blue, and amido black 10B were analyzed, and the changes in absorbance values at 465, 664, and 618 nm were chosen as indicators of the removal rates of methyl orange, methylene blue, and amido black 10B, respectively. The removal rate (R) and adsorption capacity (q) were used to evaluate the removal effect of the adsorbent on the target pollutants. First, solutions (2 L) of methyl orange, methylene blue, and amido black 10B were prepared, and their absorbances were measured by sampling. Then, 300 mL of the target solution with the adsorbent was placed in a conical flask, sealed, and placed in a constant-temperature water bath oscillator, where the adsorption experiment was performed under strict light protection conditions. After a certain period, the absorbance of the filtrate was measured, and the concentration C_t of the filtrate was calculated. The relevant calculation methods are shown in Formulas (1)–(3).

$$R = \frac{C_0 - C_t}{C_0} \times 100\%, \quad (1)$$

$$q_t = \frac{(C_0 - C_t) \times V}{m}, \quad (2)$$

$$q_e = \frac{(C_0 - C_e) \times V}{m}, \quad (3)$$

where C_0 is the concentration of the target pollutant in the solution before adsorption, mg/g; C_t is the concentration of the target pollutant in the solution at time t, mg/g; V is the volume of the reaction solution, L; m is the mass of added adsorbent used for adsorption, g; q_e is the equilibrium adsorption capacity, mg/g; q_t is the equilibrium adsorption capacity at a certain moment, mg/g; and C_e is the concentration of the target pollutant in the solution at adsorption equilibrium.

2.3. Photocatalytic Experiments

The light source, a 175 W mercury lamp (central wavelength: 365 nm), was placed at a distance from the liquid surface in the reactor. The light source was turned on about 10 min before the reaction started; 300 mL of the target pollutant solution with a certain concentration was placed in a double glass beaker, an appropriate amount of the catalyst was added to it, and the cooling water pump, magnetic stirrer, and light source were turned on for the photocatalytic experiment. The absorbance of the filtrate was measured after filtering through a 0.45 μm microporous filter membrane after sampling at certain intervals. The solution concentration after catalytic degradation was calculated according to the standard curve. The removal rate R was selected as the evaluation index for the photocatalytic degradation of target pollutants; it was calculated using Equation (1).

3. Results and Discussion

3.1. Removal of Methyl Orange, Methylene Blue, and Amido Black 10B by Zinc Ferrite

3.1.1. Removal of Methyl Orange, Methylene Blue, and Amido Black 10B by Purified Zinc Ferrite

Adsorption experiments were conducted using 300 mL of dye solutions with an initial concentration of 40 mg/L at different natural pH values (methyl orange, pH 6.5; methylene blue, pH 6.0; amido black 10B, pH 6.8) for 240 min. The results for different dosages (0.5, 1, 2, 3, 4, and 6 g/L) of purified zinc ferrite are shown in Figure 1.

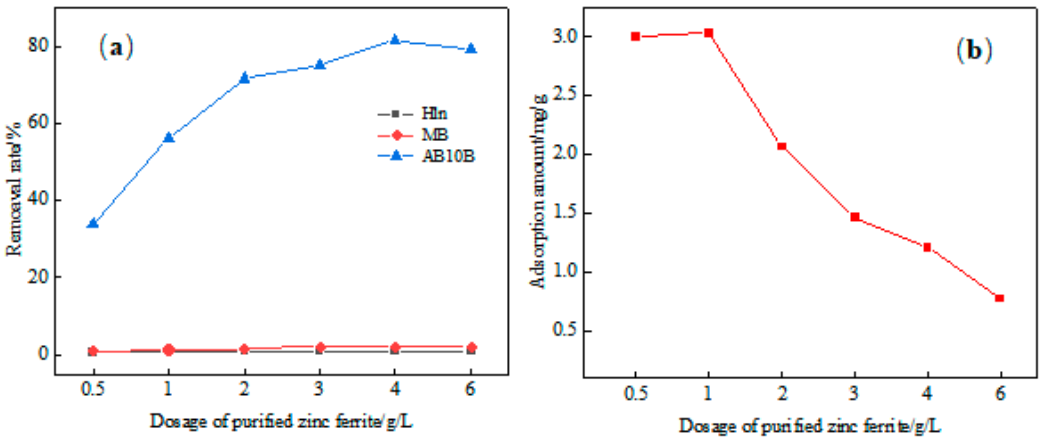

Figure 1. (**a**) Removal of different dyes by purified zinc ferrite; (**b**) the adsorption capacity of purified zinc ferrite for amido black 10B.

As shown in Figure 1a, the removal rates of methyl orange, methylene blue, and amido black 10B are ~1%, ~2%, and 81.62%, respectively. Thus, zinc ferrite exhibits certain selectivity in the removal of different dyes. In terms of Figure 1b, the highest adsorption capacity is 2.9993 mg/g, and the lowest adsorption capacity is only 0.7764 mg/g.

3.1.2. Removal of Methyl Orange, Methylene Blue, and Amido Black 10B by Synthetic Zinc Ferrite

Here, the dosages of synthetic zinc ferrite were 0.5, 1.0, 2.0, 4.0, and 6.0 g/L; the other conditions were the same as those in the experiment in Section 3.1.1. The removal rates of the three dyes by synthetic zinc ferrite calcined at different temperatures under the same test conditions are shown in Figure 2.

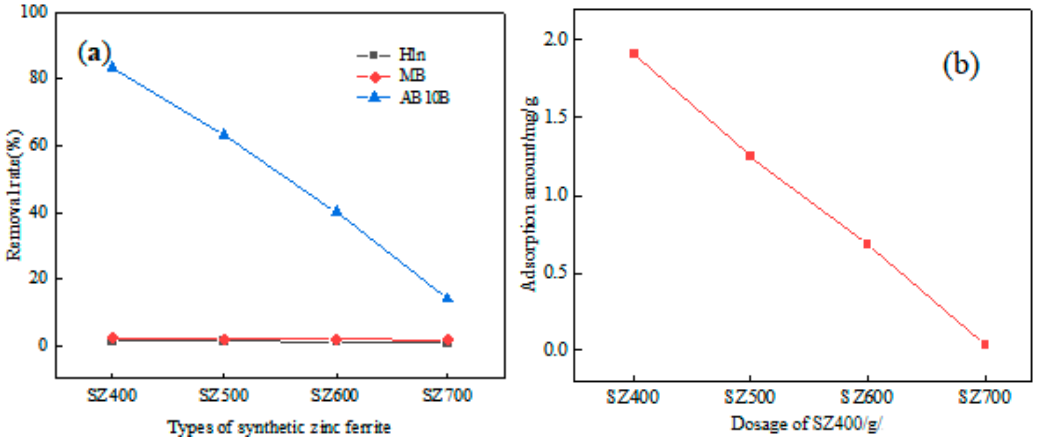

Figure 2. (**a**) Removal rates of different dyes by synthetic zinc ferrite calcined at different temperatures; (**b**) the adsorption capacity of zinc ferrite calcined at different temperatures for amido black 10B.

As shown in Figure 2a, the maximum removal rates of methylene blue and methyl orange are about 1% and 2%, respectively, while that of amido black 10B is 83.36%. Evidently, the calcination temperature of synthetic zinc ferrite significantly affects the removal of amido black 10B. In addition, the removal rate decreases with the increase in calcination temperature, ranging from 14.12% to 83.36%. As shown in Figure 2b, the adsorption capacity of zinc ferrite calcined at different temperatures for amido black 10B decreases with the increase in calcination temperature, ranging from 0.03831 to 1.9070 mg/g. Additionally, synthetic zinc ferrite calcined at 400 °C has weak crystallinity, with the peak value shifted to the left. At the same time, the lattice growth is incomplete, and the distortion, specific surface area, and pore volume of the synthetic zinc ferrite calcined at 400 °C are larger than those of zinc ferrite calcined at other temperatures. Therefore, SZ400 exhibits an optimal removal rate and adsorption capacity for amido black 10B. The calcination temperature of synthetic zinc ferrite and the amount of adsorbent both significantly affect the adsorption rates of dyes. Thus, synthetic zinc ferrite with the largest specific surface area (SZ400) was selected as the adsorbent and used in the experiment with different amounts of adsorbent. The effect of the SZ400 dosage on the removal rates of the three dyes is shown in Figure 3.

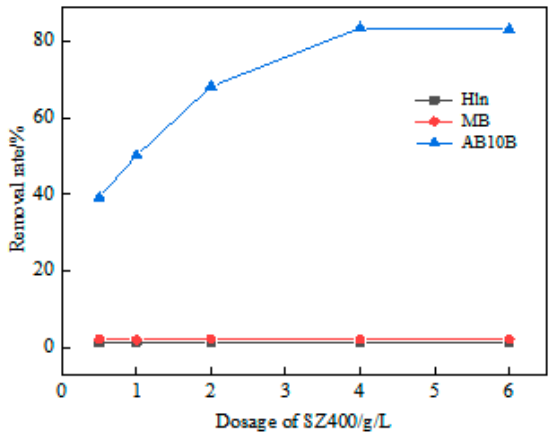

Figure 3. Effect of synthetic zinc ferrite (SZ400) dosage on the removal rates of three dyes.

As shown in Figure 3, for amido black 10B, the best removal effect is observed when the dosage of synthetic zinc ferrite is 4 g/L. Therefore, 4 g/L was selected as the optimal dosage of synthetic zinc ferrite (SZ400) for amido black 10B. Similarly, the appropriate dosages for methyl orange and methylene blue are 4 and 2 g/L, respectively.

3.1.3. Removal of Methyl Orange, Methylene Blue, and Amido Black 10B by Purchased Zinc Ferrite

The removal rates of different dyes by purchased zinc ferrite are shown in Figure 4. The other experimental conditions were the same as in the experiment in Section 3.1.1. The adsorption experiments on methyl orange, methylene blue, and amido black 10B were conducted using different dosages of purchased zinc ferrite.

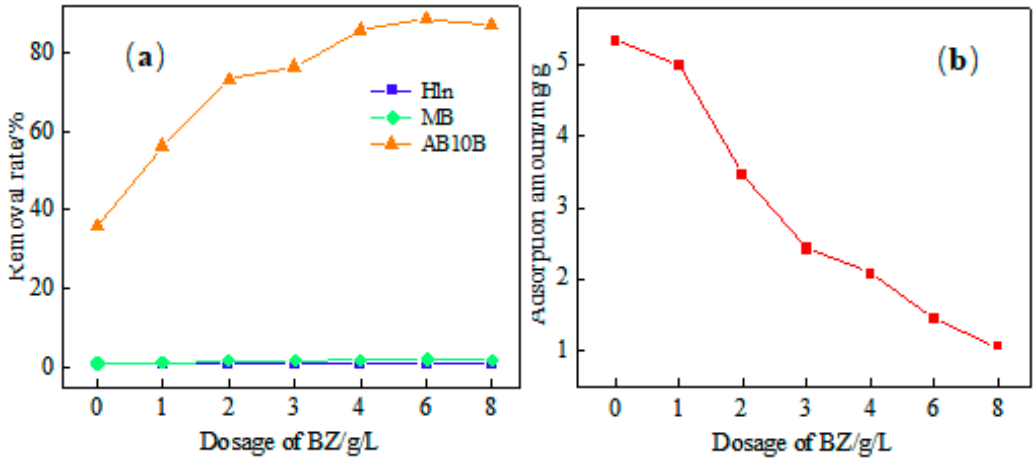

Figure 4. (**a**) Removal of different dyes by purchased zinc ferrite; (**b**) the adsorption capacity of purchased zinc ferrite for amido black 10B.

As shown in Figure 4a, the removal rates of methyl orange, methylene blue, and amido black 10B are ~1%, ~1.8%, and 88.33%, respectively. As shown in Figure 4b, the adsorption capacity of amido black 10B decreases with the increase in the dosage of purchased zinc ferrite, ranging from 1.0658 to 5.3286 mg/g.

A comparison of the removal effects of the three dyes by the three types of zinc ferrite suggests that all types of zinc ferrite show poor removal effects for methyl orange and methylene blue but better removal effects for amido black 10B. This suggests that zinc ferrite exhibits the selective removal of different dyes. The three types of zinc ferrite removed amido black 10B in the following order from the aspect of the removal rate: purchased zinc ferrite > SZ400z > purified zinc ferrite. A follow-up on how to improve the removal of amido black 10B by purified zinc ferrite requires further research.

3.2. Removal of Amido Black 10B by Purified Zinc Ferrite

3.2.1. Effect of the Particle Size of Purified Zinc Ferrite on the Removal of Amido Black 10B

The effect of the particle size of purified zinc ferrite on the removal of amido black 10B is shown in Figure 5. Purified zinc ferrite was prepared in ~150, ~75, ~38, and ~19 μm fractions. Two liters of amido black 10B solution with an initial concentration of 40 mg/L was prepared. Then, 100 mL of this solution was poured into a 250 mL conical bottle along with 1.5 g/L of purified zinc ferrites with different particle sizes. The adsorption experiment was performed at a pH of 6.8, a water bath temperature of 25 °C, and an oscillation speed of 180 rpm. At certain intervals, 3.3 mL of the adsorption solution was extracted and filtered through a 0.45 μm filter membrane. The absorbance of the obtained filtrate was measured, and the removal rate of amido black 10B was calculated.

As shown in Figure 5, when purified zinc ferrite was pulverized and not screened, the removal rate of amido black 10B was poor (only 25.91%), which was attributed to the larger overall particle size and smaller total area of purified zinc ferrite after pulverization. The removal rate by the ~150 μm fraction is significantly higher (54.1%). The removal rate reaches 58.8% at ~75 μm, 67.79% at ~38 μm, and 58.62% at ~19 μm. The results indicate that the particle size of purified zinc ferrite affects the removal of amido black 10B. With the

continuous reduction in particle size, the removal rate gradually increases until reaching a certain value, after which it no longer increases.

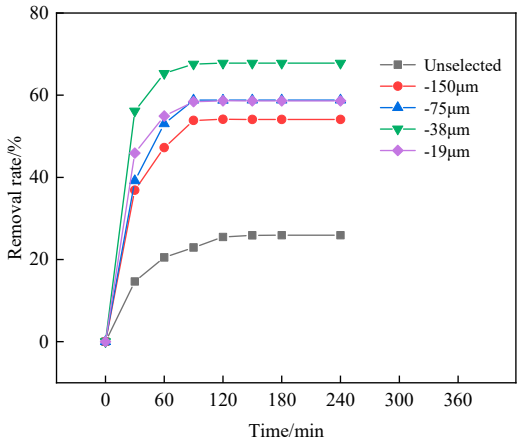

Figure 5. Effect of purified zinc ferrite particle size on the removal of amido black 10B.

3.2.2. Effect of the Dosage of Purified Zinc Ferrite on the Removal of Amido Black 10B

The effect of the dosage of purified zinc ferrite on the removal of amido black 10B is shown in Figure 6. The amido black 10B solution (300 mL) was poured into a 500 mL conical flask, and 0.5, 1, 2, 3, 4, or 6 g/L of purified zinc ferrite was added. Other conditions were the same as in the experiment in Section 3.2.1.

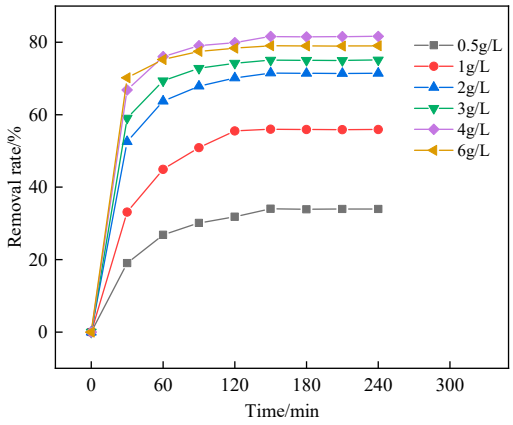

Figure 6. Effect of purified zinc ferrite dosage on the adsorption of amido black 10B.

As shown in Figure 6, within a certain range of purified zinc ferrite dosages, the removal rate of amido black 10B gradually increases with the dosage of purified zinc ferrite. This is because, with the increase in the dosage of purified zinc ferrite, the contact area, as well as the number of channels and adsorption sites, increases, thereby increasing the removal rate of amido black 10B. When the dosage of zinc ferrite is 4 g/L, the removal rate of amido black 10B reaches 81.62%. However, with a further increase in the dosage of purified zinc ferrite to 6 g/L, the removal rate of amido black 10B does not increase, possibly limited by the amount of amido black 10B in the solution. Thus, with the increase in the zinc ferrite dosage, the unit adsorption capacity steadily decreases.

3.2.3. Effect of the Physical Mixing of Purified Zinc Ferrite with Titanium Dioxide on the Removal of Amido Black 10B

Effect of Titanium Dioxide Calcined at Different Temperatures

The effect of the addition of titanium dioxide calcined at different temperatures on the removal rate of amido black 10B is shown in Figure 7. Titanium dioxide calcined at 300,

400, 500, 600, and 700 °C was added at dosages of 1, 2, 3, and 4 g/L. Other conditions were the same as in the experiment in Section 3.2.2.

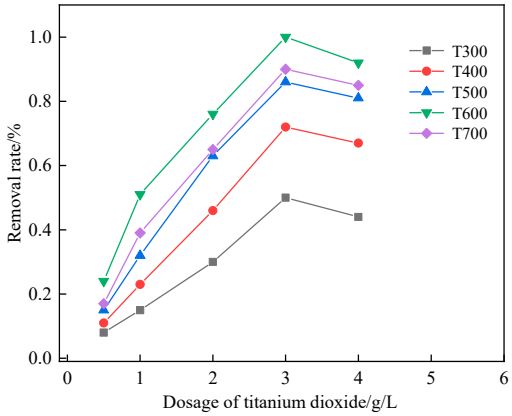

Figure 7. Effect of titanium dioxide calcined at different temperatures on the removal rate of amido black 10B.

As shown in Figure 7, the removal of amido black 10B by titanium dioxide prepared at different calcination temperatures reaches a maximum value of 1% for titanium dioxide calcined at 600 °C and only 0.4% for that calcined at 300 °C. Changes in the amount of titanium dioxide did not significantly affect the removal effect on amido black 10B, indicating that titanium dioxide used as an adsorbent had no removal effect on amido black 10B.

Under the same experimental conditions, 0.5 g/L purified zinc ferrite and 0.5 g/L titanium dioxide calcined at different temperatures were successively added to the dye solution, and the absorption experiments were repeated. The effect of the physical mixing of purified zinc ferrite with titanium dioxide calcined at different temperatures on the removal of amido black 10B is shown in Figure 8.

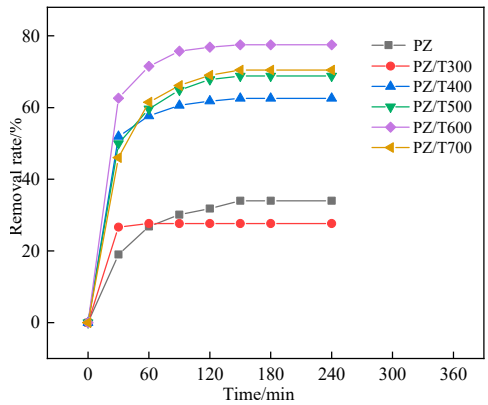

Figure 8. Effect of physical mixing of purified zinc ferrite and titanium dioxide calcined at different temperatures on the removal of amido black 10B.

As shown in Figure 8, titanium dioxide, except for that prepared at 300 °C, promoted the removal of amido black 10B by purified zinc ferrite. The removal rate of amido black 10B increased from 28.54% to 43.49%; that is, the mixing of titanium dioxide and zinc ferrite produced a synergistic effect. Additionally, titanium dioxide calcined at 600 °C showed the best performance, increasing the removal rate of amido black 10B by 43.49% to 77.51%. T300 possesses the largest specific surface area, the worst crystallinity, and the smallest grain size, whereas T600 has the smallest specific surface area, the highest crystallinity, and the largest grain size. The obtained results show that the synergistic effect of zinc ferrite

and titanium dioxide may be affected by the grain size, specific surface area, microstructure, crystallinity, and other factors.

Effect of the Titanium Dioxide Dosage

According to the results presented in Section 3.1.2, the removal effect on amido black 10B is the best when the dosage of purified zinc ferrite is 4 g/L, and the best synergistic adsorption effect is attained when using T600 and purified zinc ferrite. The effect of the titanium dioxide dosage on the removal of amido black 10B by purified zinc ferrite is shown in Figure 9. The dosage of purified zinc ferrite was 4 g/L, and the dosages of T600 were 0.5, 1, 2, and 3 g/L. Other conditions were the same as those in the experiment in Section 3.2.2.

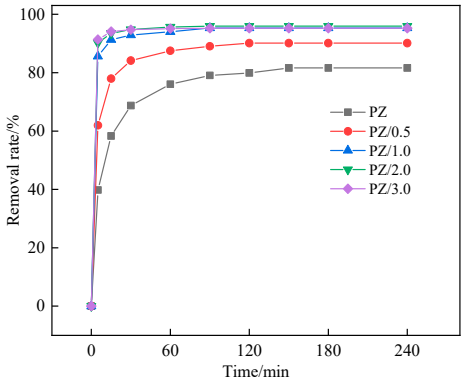

Figure 9. Effect of the titanium dioxide dosage on the removal of amido black 10B by purified zinc ferrite.

As shown in Figure 9, when the dosage of T600 was only 0.5 g/L, the removal rate of amido black 10B after 5 min increased by 22.2% to 61.94%. After 30 min, the removal rate increased by 15.4% to 84.13%. When the dosage reached 3 g/L, the removal rate after 5 min increased by 51.6% to 91.37%. After 30 min, the removal rate increased by 25.99% to 94.72%. Therefore, the addition of a small amount of T600 can promote the removal of amido black 10B by zinc ferrite. Therefore, 2–3 g/L was considered the optimal dosage of titanium dioxide.

Effect of the Initial pH of the Solution

The effect of the initial pH of the amido black 10B solution on the removal rate is shown in Figure 10. The pH of the amido black 10B solution was adjusted to 3, 5, 6.8 (natural pH value), 9, and 11, and the dosages of purified zinc ferrite and T600 were 4 and 3 g/L, respectively. Other conditions were the same as those in the experiment in Section 3.2.2.

The effect of the initial pH of the amido black 10B solution on the removal rate is shown in Figure 10. Amido black 10B is an alkaline dye. Under acidic conditions, the positive charge on the surface of the mixture of purified zinc ferrite and titanium dioxide increases, which increases the electrostatic attraction to the surface of the mixture to a certain extent and improves the electrostatic adsorption of amido black 10B, thereby increasing the removal rate. When the initial pH value of the solution increases, the number of OH^- ions in the solution also increases, and the positive charge on the surface of the mixture decreases, leading to a corresponding decrease in adsorption and the removal rate. The mixture of purified zinc ferrite and titanium dioxide maintains high catalytic activity in acidic to weakly alkaline solutions, but its activity slightly decreases in alkaline solutions.

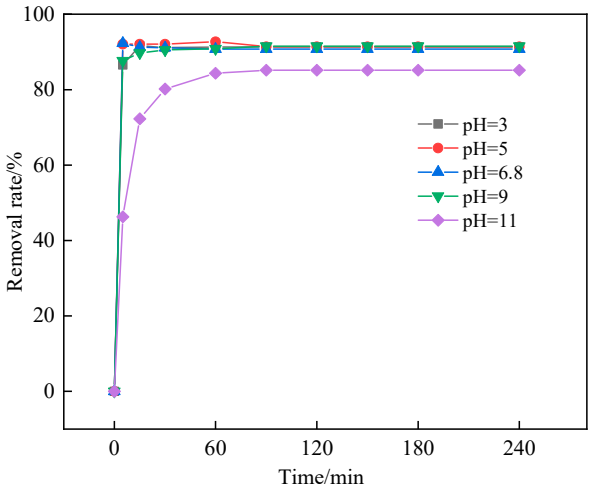

Figure 10. Effect of the initial pH of amido black 10B solution on the removal rate.

3.2.4. Effect of Time

The effect of time on the removal rate of amido black 10B is shown in Figure 11. Adsorption experiments were conducted in conical bottles using 4 g/L purified zinc ferrite, SZ400, and purchased zinc ferrite, as well as 4 g/L purified zinc ferrite and 3 g/L T600 as adsorbents. The adsorption times were 5, 15, 30, 60, 90, 120, 150, 180, and 240 min; other conditions were the same as those in the experiment in Section 3.2.2.

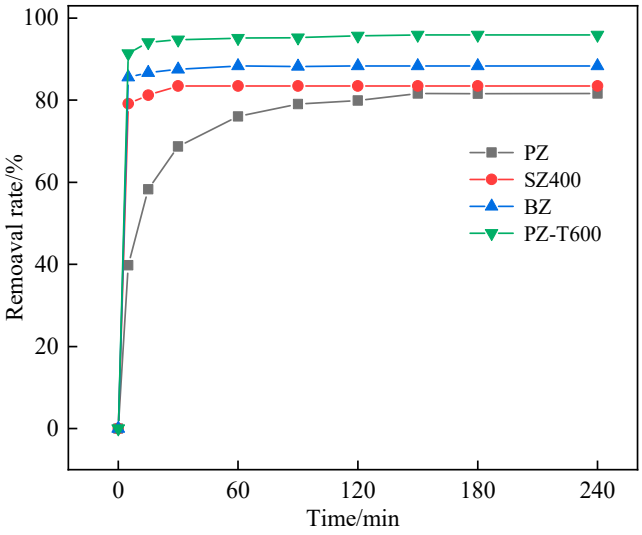

Figure 11. Effect of time on the removal rate of amido black 10B.

As shown in Figure 11, the removal rates of amido black 10B by SZ400 and purchased zinc ferrite increased quickly and tended to reach equilibrium after 30 min, reaching 83.47% and 88.31%, respectively. When purified zinc ferrite was added alone, the removal of amido black 10B reached equilibrium after 150 min, with a removal rate of 81.60%. In contrast, when using the mixture of purified zinc ferrite with titanium dioxide, the removal rate of amido black 10B increased faster and tended to balance at 95.89% after 30 min. This indicates that mixing zinc ferrite with titanium dioxide effectively improves the removal rate of amido black 10B and shortens the equilibrium time.

3.3. Effect of Zinc Ferrite on the Photocatalytic Degradation of Methylene Blue

Since different types of zinc ferrite have almost no adsorption effect on methylene blue, the photocatalytic performance of zinc ferrite was used, and the effect on the photocatalytic degradation of methylene blue was explored.

3.3.1. Effect of Purified Zinc Ferrite Dosage

The effect of the amount of purified zinc ferrite on the photocatalytic removal of methylene blue is shown in Figure 12. The methylene blue solution (300 mL) with an initial concentration of 20 mg/L was placed in a 500 mL double glass beaker, and 0.05, 0.1, 0.15, 0.20, 0.25, or 0.30 g of the purified zinc ferrite catalyst was added. The pH value of the solution was the natural pH value (6.0). After sampling and filtering, the absorbance was measured, and the photocatalytic experiment was performed. After the photocatalytic reaction occurred for a certain period, the absorbance of the supernatant was measured, and the removal rate of methylene blue was calculated.

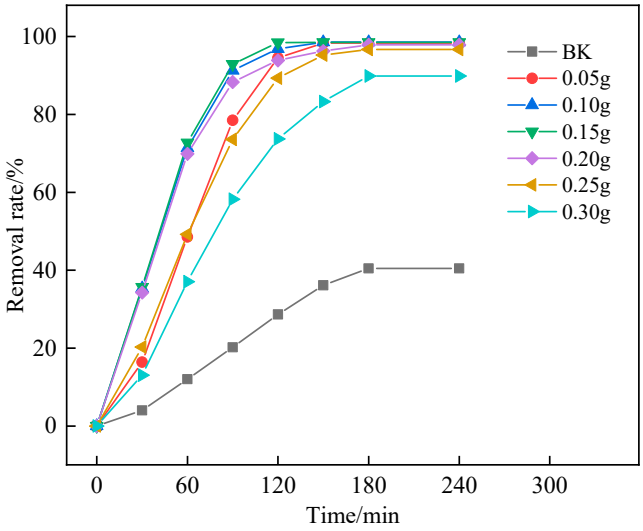

Figure 12. Effect of purified zinc ferrite dosage on the photocatalytic removal of methylene blue.

As shown in Figure 12, at dosages of purified zinc ferrite between 0.1 and 0.2 g, the photocatalytic degradation of methylene blue improved with the increase in the dosage of purified zinc ferrite. However, when the dosage of the catalyst was increased to 0.3 g, the removal rate significantly decreased. When the dosage of the catalyst is small, its contact area with methylene blue is also small. With the increase in the amount of purified zinc ferrite, the contact area increases, making full use of the energy of incident light, resulting in a significant increase in photocatalytic efficiency. However, at excessive catalyst dosages, the light is scattered to a certain extent, causing the wastage of the catalyst. Therefore, 0.15 g was selected as the optimal catalyst dosage.

3.3.2. Effect of the Initial Concentration of the Solution

The effect of the initial solution concentration on the photocatalytic degradation of methylene blue by purified zinc ferrite is shown in Figure 13. After weighing 0.15 g of purified zinc ferrite, methylene blue solutions with initial concentrations of 10, 20, 30, and 40 mg/L were prepared, and photocatalytic experiments were performed. Other conditions were the same as those in the experiment in Section 3.3.1.

As shown in Figure 13, within a certain concentration range, the photocatalytic performance of purified zinc ferrite on methylene blue is weakly affected by the initial solution concentration. At initial methylene blue concentrations of 10–30 mg/L, the removal rates of methylene blue are above 95% after 120 min of photocatalysis. However, at a methylene blue concentration of 40 mg/L, the removal rate is only 24.88% at 120 min and 77.01% at 240 min. The photocatalytic reaction occurs on the active sites on the surface of the catalyst; therefore, with a constant amount of the catalyst, there is a certain dynamic balance between the catalyst and the dye. At the same time, the increase in the dye concentration gradually disrupts this balance and reduces the removal rate. When it reaches a certain value, the balance is destroyed, resulting in a considerable decrease in the removal rate.

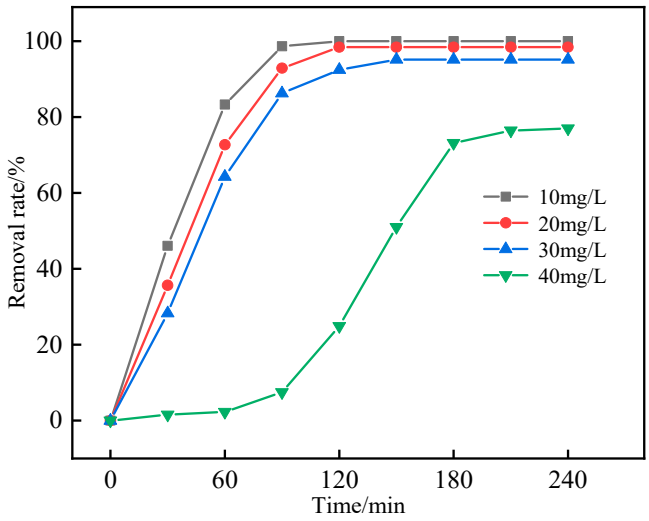

Figure 13. Effect of initial solution concentration on the photocatalytic degradation of methylene blue by purified zinc ferrite.

3.3.3. Effect of Solution pH

The effect of the initial solution pH on the photocatalytic removal of methylene blue by zinc ferrite is shown in Figure 14. The initial pH of the methylene blue solution was adjusted to 3, 4, 5, 6 (natural pH), 7, 8, 9, 10, and 11, and 0.15 g of the purified zinc ferrite catalyst was used. Other conditions were the same as those in the experiment in Section 3.3.1.

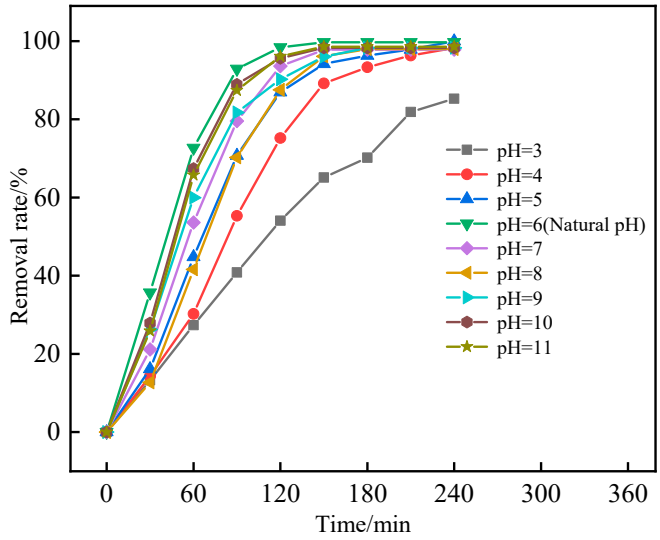

Figure 14. Effect of the initial solution pH on the photocatalytic removal of methylene blue by purified zinc ferrite.

As shown in Figure 14, at a solution pH of 3, the removal rate of methylene blue by purified zinc ferrite was only 65.13% after 150 min of illumination. However, in weakly acidic or alkaline solutions, pH had little effect on the photocatalytic degradation of methylene blue, and the removal rate was >94% after 150 min of photocatalytic degradation. Additionally, at the natural solution pH of 6.0, the photocatalytic effect of purified zinc ferrite on methylene blue is the best. Under these conditions, the removal rate of methylene blue reached 92.91% after photocatalytic degradation for 90 min and 99.70% after 150 min. This indicates that purified zinc ferrite exhibits higher photocatalytic degradation activity toward methylene blue under neutral, weakly acidic, and alkaline conditions.

3.3.4. Comparison of the Photocatalytic Performance of Different Types of Zinc Ferrite toward Methylene Blue

The effect of the type of zinc ferrite on the removal rate of methylene blue is shown in Figure 15. The dosage of the zinc ferrite photocatalyst was 0.15 g, and other conditions were the same as those in the experiment in Section 3.3.1.

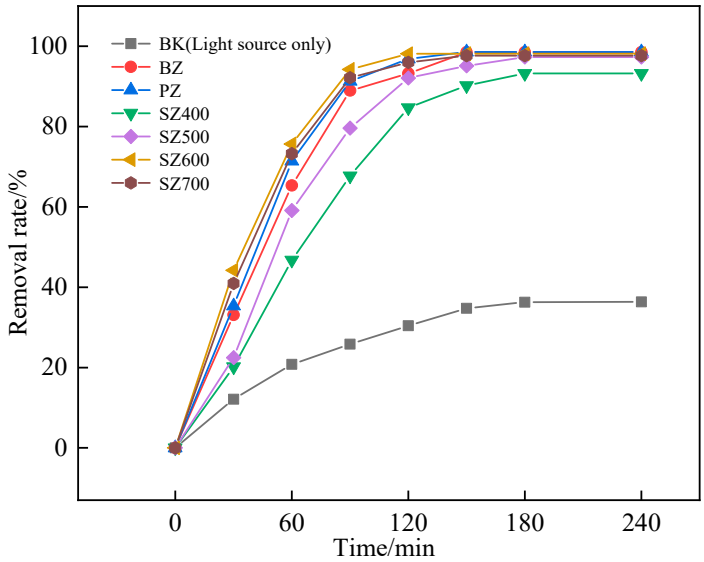

Figure 15. Effect of the type of zinc ferrite on the removal rate of methylene blue.

As shown in Figure 15, under light irradiation without a catalyst, the removal rate of methylene blue is only 12.13% at 30 min and 36.35% at 180 min. In the presence of different types of zinc ferrite as catalysts, the removal rates are significantly higher. For example, the removal rate of methylene blue after 30 min of photocatalysis is increased by 8.08–32.09% with the addition of synthetic zinc ferrite. In the presence of purified zinc ferrite and purchased zinc ferrite, the removal rates are 23.20% and 20.97% higher, respectively, than in the case without a catalyst. After 180 min of photocatalysis, the removal rate of synthetic zinc ferrite is 56.93–61.84% higher than without a catalyst. With purified zinc ferrite, the removal rate is 62.28% higher, and with purchased zinc ferrite, it is 62.22% higher than without a catalyst.

Overall, purchased zinc ferrite possesses the largest specific surface area and the strongest absorption of ultraviolet light, but the worst crystallinity. Purified zinc ferrite has the smallest specific surface area and medium light absorption, but its crystallinity is the best, so the difference between their removal rates is small. Considering synthetic zinc ferrite, the one calcined at 400 °C has a large specific surface area but poor crystallinity and the weakest absorption of ultraviolet light; thus, it shows the smallest improvement in the methylene blue degradation rate. Synthetic zinc ferrite calcined at 600 °C has better crystallinity, larger specific surface area, and stronger absorption of ultraviolet light, thereby resulting in the largest improvement in the removal rate. Therefore, the photocatalytic performance of zinc ferrite is affected by its specific surface area, crystallinity, and microstructure.

3.4. Effect of Zinc Ferrite on the Photocatalytic Degradation of Methyl Orange

Since different types of zinc ferrite have almost no adsorption effect on methyl orange, the photocatalytic performance of zinc ferrite was used, and the effect on the photocatalytic degradation of methyl orange was explored.

3.4.1. Effect of the Type of Zinc Ferrite

The effect of the type of zinc ferrite on the photocatalytic degradation of methyl orange is shown in Figure 16. A solution of methyl orange (2 L) with an initial concentration of 20 mg/L and pH of 6.5 was prepared; 300 mL of this solution was placed in a double-layer glass beaker, and its absorbance was measured by sampling. Then, 0.15 g of purified zinc ferrite, synthetic zinc ferrite prepared at different calcination temperatures, and purchased zinc ferrite were added as catalysts for the photocatalytic reaction experiment. After filtering, the absorbance was measured, and the removal rate of methyl orange was calculated.

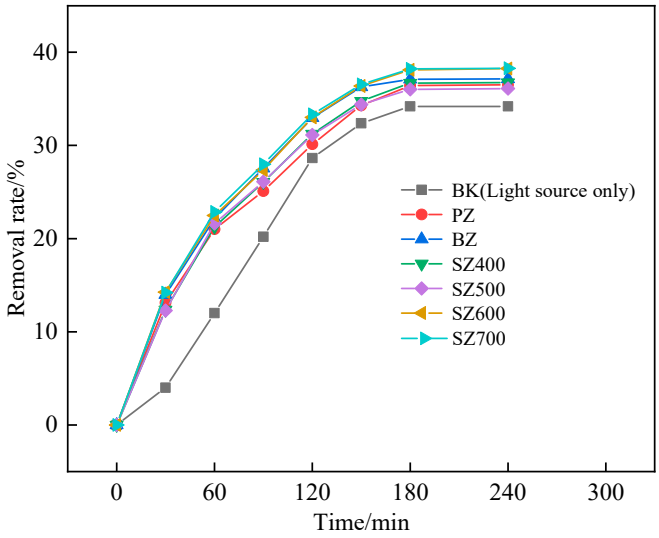

Figure 16. Relationship between lnK_L and 1/T.

As shown in Figure 16, the addition of different types of zinc ferrite did not significantly improve the removal rate of methyl orange. With the use of these catalysts, the removal rate is between 36.12 and 38.28%, corresponding to an increase of 1.93–4.09% over the case without a catalyst. These results indicate that the three kinds of zinc ferrite do not significantly promote the photocatalytic degradation of methyl orange.

3.4.2. Effect of the Amount of Zinc Ferrite/Titanium Dioxide

In this experiment, 0.05, 0.1, 0.15, and 0.20 g T400/PZ (5%) were used as the catalyst, and the other conditions were the same as those in the experiment in Section 3.4.1. The effect of T400/PZ (5%) on the photocatalytic activity of methyl orange is shown in Figure 17.

As shown in Figure 17, the best photocatalytic degradation effect on methyl orange is observed at a T400/PZ (5%) dosage of 0.15 g. We speculate that at a low dosage of the catalyst, the contact area with methyl orange is small, and at an excessive dosage of the catalyst, the catalyst has a certain scattering effect on light. Therefore, 0.15 g was considered the optimal dosage of T400/PZ (5%).

3.4.3. Effect of the Initial Solution Concentration

The effect of the initial solution concentration on the degradation of methyl orange by T400/PZ (5%) is shown in Figure 18. The experiment was performed in a 500 mL double-layer glass beaker with 0.15 g of T400/PZ (5%) and methyl orange solutions with initial concentrations of 10, 20, 25, and 30 mg/L. Other conditions were the same as those in the experiment in Section 3.4.1.

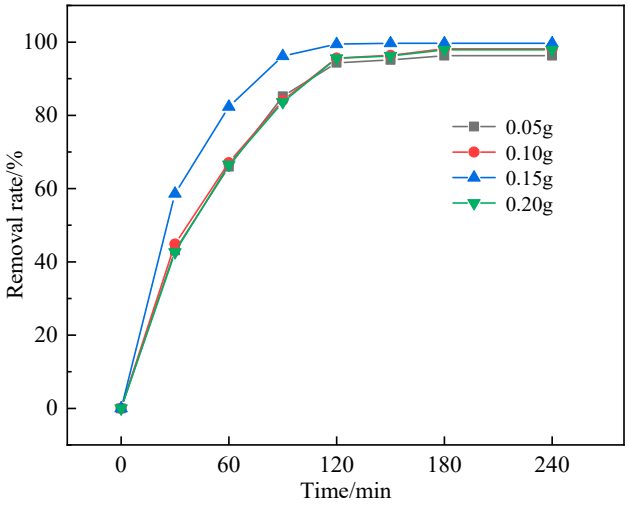

Figure 17. Effect of the amount of zinc ferrite/titanium dioxide composite catalyst on the photocatalytic degradation of methyl orange.

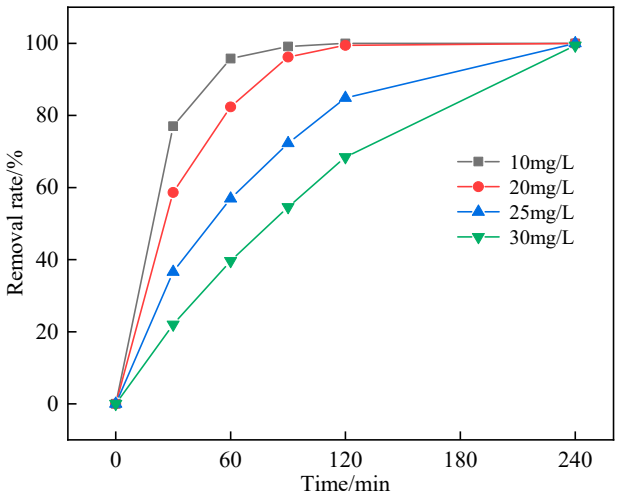

Figure 18. Effect of initial solution concentration on the photocatalytic degradation of methyl orange by the zinc ferrite/titanium dioxide mixture.

As shown in Figure 18, within a certain concentration range, the photocatalytic removal rate of methyl orange is not significantly affected by the initial solution concentration. At initial methyl orange concentrations of 10–20 mg/L, the removal rate reaches 99% after 120 min of photocatalysis. However, with the increase in methyl orange concentration to 25 mg/L, the removal rate decreases to 84.85% after 120 min. At 30 mg/L, the removal rate is only 68.43% after 120 min. This is explained as follows. The photocatalytic reaction occurs on the active sites on the catalyst surface. With a certain amount of catalyst in the system, a dynamic reaction balance between the catalyst and methyl orange is established. Increasing the concentration of methyl orange gradually disrupts this balance and reduces the degradation rate. Above a certain concentration, the balance is destroyed, leading to a significant decrease in the degradation rate of methyl orange.

3.4.4. Effect of Titanium Dioxide

The dosage of the zinc ferrite and titanium dioxide composite photocatalyst was 0.15 g. Different titanium dioxide catalysts were used to determine the effect of the type of titanium dioxide on the photocatalytic degradation of methyl orange. Other conditions were the same as those in the experiment in Section 3.4.1. The results are shown in Figure 19.

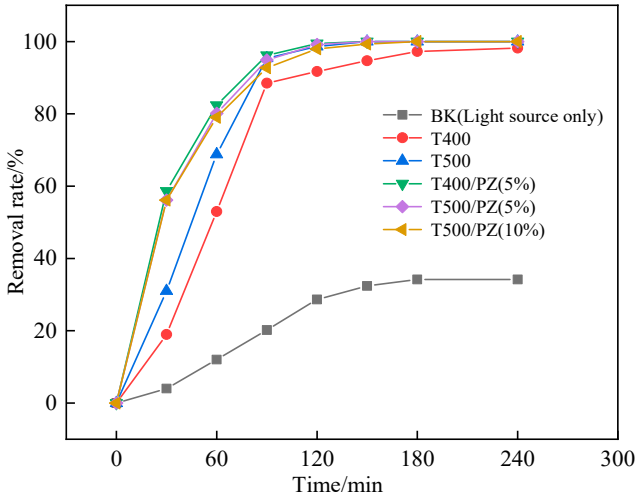

Figure 19. Effect of different types of titanium dioxide on the photocatalytic degradation of methyl orange.

As shown in Figure 19, synthetic titanium dioxide exhibits a good photocatalytic performance for methyl orange, and its combination with purified zinc ferrite exhibits even better photocatalytic performance. The removal rate of methyl orange increased from 29.38% to 82.35% after 60 min of photocatalysis. After 120 min of photocatalysis, the removal rate increased by 7.73% to 99.44%. Considering the calcination temperature of titanium dioxide, when used alone, titanium dioxide prepared at 500 °C shows the best photocatalytic effect. However, when used along with purified zinc ferrite, titanium dioxide calcined at 400 °C shows better results.

4. Conclusions

(1) The highest removal rates of amido black 10B by the three zinc ferrites ranged from 81.62% to 88.33%; those of methyl orange and methylene blue were about 1% and about 2%, respectively.

(2) Titanium dioxide (0.5 g/L) prepared at different calcination temperatures was physically mixed with purified zinc ferrite (0.5 g/L) to improve the adsorption of amido black 10B (40 mg/L). The best removal effect was observed when using titanium dioxide calcined at 600 °C, and the removal rate of amido black 10B increased from 43.49% to 77.51%.

(3) The optimal conditions for the photocatalytic degradation of methylene blue by zinc ferrite were as follows: a zinc ferrite catalyst dosage of 0.15 g, an initial solution concentration of 20 mg/L, and a pH of 6.0.

(4) The photocatalytic degradation rate of methyl orange reached 100% after 180 min at the following optimal conditions: a zinc ferrite and titanium dioxide composite catalyst dosage of 0.15 g, an initial dye solution concentration of 20 mg/L, and a pH of 6.5.

Author Contributions: Conceptualization, J.Y. and S.M.; data curation, Z.L. and J.Y.; formal analysis, H.L. and T.W.; funding acquisition, J.Y.; investigation, T.W. and H.L.; methodology, J.Y. and S.M.; project administration, J.Y. and S.M.; validation, H.L. and J.Y.; writing—original draft, X.H. and J.Y.; writing—review and editing, J.Y. and X.H. All authors have read and agreed to the published version of the manuscript.

Funding: This research was funded by the National Natural Science Foundation of China (No. 52264020, No. 51774099).

Data Availability Statement: Not applicable.

Conflicts of Interest: The authors declare no conflict of interest.

References

1. Liu, X.; Yang, Y.; Shi, X.; Li, K. Fast photocatalytic degradation of methylene blue dye using a low-power diode laser. *J. Hazard. Mater.* **2015**, *283*, 267–275. [CrossRef] [PubMed]
2. Fatima, M.; Farooq, R.; Lindström, R.W.; Saeed, M. A review on biocatalytic decomposition of azo dyes and electrons recovery. *J. Mol. Liq.* **2017**, *246*, 275–281. [CrossRef]
3. Mo, J.H.; Lee, Y.H.; Kim, J.; Jeong, J.Y.; Jegal, J. Treatment of dye aqueous solutions using nanofiltration polyamide composite membranes for the dye wastewater reuse. *Dye. Pigment.* **2008**, *76*, 429–434. [CrossRef]
4. Greluk, M.; Hubicki, Z. Evaluation of polystyrene anion exchange resin for removal of reactive dyes from aqueous solutions. *Chem. Eng. Res. Des.* **2013**, *91*, 1343–1351. [CrossRef]
5. Gong, Z.; Fu, T.Y.; Sun, H.F.; Zhao, X.; Cheng, Z.; Li, J. Research progress on treatment of printing and dyeing wastewater by advanced oxidation Technology. *Hydrometall. China* **2022**, *41*, 283–288.
6. Azbar, N.; Yonar, T.; Kestioglu, K. Comparison of various advanced oxidation processes and chemical treatment methods for COD and color removal from a polyester and acetate fiber dyeing effluent. *Chemosphere* **2004**, *55*, 35–43. [CrossRef]
7. Bai, W.Q. Study on Advanced Treatment of Printing and Dyeing Wastewater by Micro Electrolysis-Fenton Oxidation Combined with Biological Treatment. Master's Thesis, Nanjing Agricultural University, Nanjing, China, 2017.
8. Huang, W.; Cao, X.J.; Zhu, H.Z.; Tang, B.M. Research on physic adsorption and photocatalytic activity of TiO_2/SiO_2 with different molar content of SiO_2. *J. Wuhan Univ. Technol.* **2015**, *37*, 25–31.
9. Spagni, A.; Casu, S.; Grilli, S. Decolourisation of textile wastewater in a submerged anaerobic membrane bioreactor. *Bioresour. Technol.* **2012**, *117*, 180–185. [CrossRef] [PubMed]
10. Liu, N.; Zheng, X.L.; Xie, X.H.; Sun, P.; Wang, L.; Su, H.M. Effect of oxygen on decolorization and degradation of azo dyes by mixed flora. *Microbiol. China* **2020**, *47*, 2359–2371.
11. Tomei, M.C.; Pascual, J.S.; Angelucci, D.M. Analysing performance of real textile wastewater bio-decolourization under different reaction environments. *J. Clean. Prod.* **2016**, *129*, 468–477. [CrossRef]
12. Qin, B.; Gu, J.C.; Yin, P. Research progresses on dye wastewater treatment technology. *Environ. Prot. Chem. Ind.* **2021**, *41*, 9–18.
13. Xu, W.F.; Sun, L.; Yuan, X.J.; Xia, D.S. Preparation of nanometer zinc ferrite and its application in water treatment. *Technol. Water Treat.* **2020**, *46*, 6–10.
14. Lemine, O.M.; Bououdina, M.; Sajieddine, M.; AAl-Saie, M.; Shafi, M.; Khatab, A.; Al-hilali, M.; Henini, M. Synthesis, structural, magnetic and optical properties of nanocrystalline $ZnFe_2O_4$. *Phys. B Condens. Matter* **2011**, *406*, 1989–1994. [CrossRef]
15. Fan, G.; Gu, Z.; Yang, L.; Li, F. Nanocrystalline zinc ferrite photocatalysts formed using the colloid mill and hydrothermal technique. *Chem. Eng. J.* **2009**, *155*, 534–541. [CrossRef]
16. Cai, C.; Zhang, Z.; Liu, J.; Shan, N.; Zhang, H.; Dionysiou, D.D. Visible light-assisted heterogeneous Fenton with $ZnFe_2O_4$ for the degradation of Orange II in water. *Appl. Catal. B Environ.* **2016**, *182*, 456–468. [CrossRef]
17. Savunthari, K.V.; Shanmugam, S. Effect of co-doping of bismuth, copper and cerium in zinc ferrite on the photocatalytic degradation of bisphenol A. *J. Taiwan Inst. Chem. Eng.* **2019**, *101*, 105–118. [CrossRef]
18. Li, P.; Liu, Y.; Xue, R.; Fan, X. Magnetic retrievable $Ag/AgBr/ZnFe_2O_4$ photocatalyst for efficient removal of organic pollutant under visible light. *Appl. Organomet. Chem.* **2020**, *34*, e5548. [CrossRef]
19. Yang, J.; Huo, X.; Li, Z.; Ma, S. Study on properties of zinc ferrite, titanium dioxide and their composites. *E3S Web Conf.* **2023**, *385*, 04016. [CrossRef]